8c

2164

LA-4935-MS

Pulsed Piezoresistive Gauge Bridge

los alamos
scientific laboratory
of the University of California
LOS ALAMOS, NEW MEXICO 87544

UNITED STATES
ATOMIC ENERGY COMMISSION
CONTRACT W-7405-ENG. 36

Printed in the United States of America. Available from
National Technical Information Service
U. S. Department of Commerce
5285 Port Royal Road
Springfield, Virginia 22151
Price: Printed Copy $3.00; Microfiche $0.95

LA-4935-MS
UC-37 & UC-40
ISSUED: May 1972

los alamos
scientific laboratory
of the University of California
LOS ALAMOS, NEW MEXICO 87544

Pulsed Piezoresistive Gauge Bridge

by

Ralph R. Fullwood

PULSED PIEZORESISTIVE GAUGE BRIDGE

by

Ralph R. Fullwood

ABSTRACT

This paper describes a piezoresistive gauge bridge operating in a NIM configuration. It achieves a sensitivity of 1 or 0.5V/% resistance change by using a pulse of 200 or 100 V respectively, to interrogate the gauge. A bipolar line driver capable of ± 20 V, and having a gain of 0.95 driving 50 Ω, supplies the bridge output to recording equipment. The maximum risetime of the bridge is 50 nsec, the settling time is 200 nsec, the turn-off time is 1 μsec, and the time delay following an external trigger is 400 nsec.

A mathematical analysis of the operation of the pulsed piezoresistive gauge bridge is presented with a comparison of results to calculations. The effect of remotely coupling a gauge to the bridge by a lossy transmission line is presented as well as compensation of this effect by a second equally lossy line.

I. INTRODUCTION

The sensing of piezoresistive strain transducers under the severe environmental conditions of a nuclear explosion presents problems of impedance matching, bandwidth, and signal-to-noise ratios.

An objective of the design presented here was to achieve the maximum sensitivity for a minimum pulsed voltage across the piezoresistive element. It will be shown that the results of this design are within 95% of that theoretically possible. The reason for minimizing the pulsed voltage is that there is evidence of gauge sparking and failure when subject to large pulsed voltages in a radiation environment. A further objective was to achieve an impedance matched system. This is done by "floating" the power supply that pulses the bridge so that the only impedance to ground is through the coupling transformer capacity. In this design, one side of the bridge terminates the other, hence the module has no characteristic impedance and can be used on 50, 75, or 90 Ω systems. This assumes that when the silicon control rectifier (SCR) switches close, their impedance is zero. No successful scheme has been devised to measure the possible error of this approximation, but it is believed to be a valid assumption. Previous bridge designs lost sensitivity by being fully passive. When the bridge-balance is required to drive a 50 Ω line to the recording equipment, a serious sacrifice in sensitivity must be paid. This design uses a bipolar emitter-follower driver as the output stage and is unique in that the operating point is controlled by a light-link. The electronics package is a single-width 8 3/4-in. NIM module that uses standard NIM voltages and pin connections.[1,2] The design is simplified by using medium scale TTL integrated circuit logic for control.

II. THEORY

There is a very close connection between time-domain reflectometry (TDR) and a pulsed bridge. In the case of the former, the pulses interrogating the piezoresistive element (PRE) are short bursts so that the reflection arrives at the sending end when the driving pulse is absent. In the latter case, a step-voltage is applied to the PRE; the response is compared with a reference voltage established by the other side of the bridge and the difference is related to the dynamic PRE resistance.

Referring to Fig. 1, the current I delivered into the termination R is given by the difference between the forward $\underset{\rightarrow}{I}$ and reflected pulse current $\underset{\leftarrow}{I}$; $I = \underset{\rightarrow}{I} - \underset{\leftarrow}{I}$. The pulse current and voltage are related at any intermediate point through the characteristic impedance of the transmission line Z_o

$$\underset{\rightarrow}{I} = \frac{\underset{\rightarrow}{V}}{Z_o} \; ; \; \underset{\leftarrow}{I} = \frac{\underset{\leftarrow}{V}}{Z_o} \; .$$

The voltage developed on the termination is the sum of the forward and reflected voltages $V = \underset{\leftarrow}{V} + \underset{\rightarrow}{V}$. Eliminating the current and rearranging,

$$\frac{\underset{\leftarrow}{V}}{\underset{\rightarrow}{V}} = \frac{R - Z_o}{R + Z_o} = \rho \; . \qquad (1)$$

Equation (1) is applicable at the location of R, but must be corrected for the cable propagation time to determine the relationship at the generator end

$$\frac{\underset{\leftarrow}{V}(t)}{\underset{\rightarrow}{V}(t-2\tau)} = \frac{R(t-\tau) - Z_o}{R(t-\tau) + Z_o} = \rho(t-\tau) \; , \qquad (2)$$

where τ is the one-way signal travel time in the transmission line.

Equation (2) is the idealized equation of TDR and shows that both the magnitude and distance to the discontinuity $\rho(t-\tau)$ can be determined. It is inaccurate in that it assumes an ideal line having a well-defined delay and characteristic impedance; it also assumes the line to be independent of frequency response. All of these assumptions contribute effects which are observed experimentally.

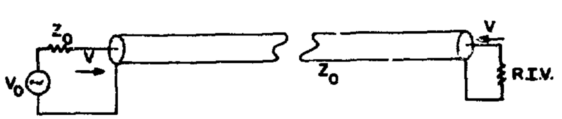

Fig. 1. The transmission line problem.

At the driving end of the line, the signal reflected by the PRE will be represented by a voltage generator having the line impedance (see Fig. 2).

It is readily seen that

$$V_c(t) = 1/2\,[V_o(t) + \underset{\leftarrow}{V}(t)] \; , \qquad (3)$$

and, as before,

$$V_c(t) = \underset{\rightarrow}{V}(t) + \underset{\leftarrow}{V}(t) \; . \qquad (4)$$

If there were no reflected wave,

$$\underset{\rightarrow}{V}(t) = 1/2\,V_o(t) \; . \qquad (5)$$

Combining Equations (2), (3), and (5) results in an equation suitable for use with TDR or pulsed-bridge sensing of piezoresistive elements.

$$V_c(t) = 1/2\,V_o(t) + 1/2\,V_o(t-2\tau)\,\rho(t-\tau) \; . \qquad (6)$$

A. Case I (TDR)

In this case, $V_o(t) = 0$, hence Eq. (6) becomes

$$V_c(t) = 1/2\,V_p\,\rho(t-\tau) \; . \qquad (7)$$

Note that if $R = Z_o$, $\rho(t-\tau) = 0$, and $V_c(t)$ is zero, hence no bridge or offset amplifier is needed.

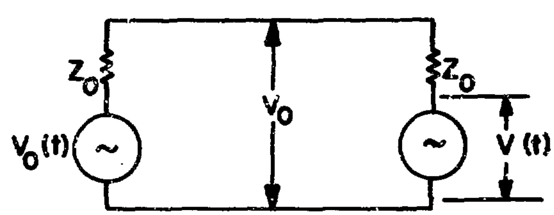

Fig. 2. An equivalent circuit for a cable and matched pulser.

B. Case II (Pulsed Bridge)

In this case, the pulsed voltage $V_o(t) = V_o$ i.e., lasts for a time longer than 2τ. Equation (6) becomes

$$V_c(t) = 1/2\ V_o\ [1 + \rho\ (t-\tau)] \quad . \qquad (8)$$

Now if $\rho = 0$, $V_c = 1/2\ V_o$ and an offset amplifier or bridge is needed to remove this pedestal.

If ρ is replaced by its definition [Eq. (1)] then

$$V_c(t) = V_o \frac{R\ (t-\tau)}{R\ (t-\tau) + Z_o} \quad . \qquad (9)$$

Equation (9) gives the same result (except for retarded time) that would have been obtained in the absence of the transmission line. We must conclude that the pulsed bridge has proper pulse propagation characteristics under the assumption of an ideal transmission line and a matched-source impedance. The application of TDR to the pulsed bridge problem is a valuable conceptual approach. It allows the visualization of the long-duration bridge pulse as being composed of many short-duration pulses at such a high repetition rate that the duty is 100%. These short duration pulses are continually being reflected from the PRE and interrogating its resistance.

If $R = Z_o + \Delta R$, where ΔR represents the change of resistance of the PRE when under stress, then Eq. (9) may be expanded in a Taylor's series

$$V_c(t) = \frac{V_o(Z_o + \Delta R)}{2\ Z_o} \left[1 - \left(\frac{\Delta R}{2\ Z_o}\right) + \left(\frac{\Delta R}{2\ Z_o}\right)^2 + \ldots\right]$$

$$= \frac{V_o\ \Delta R(t-\tau)}{4\ Z_o} \left[1 - \left(\frac{\Delta R(t-\tau)}{2\ Z_o}\right)^2 + \ldots\right] , \qquad (10)$$

where the term $V_o/2$ has been dropped as being cancelled by the bridge action.

The response of a coaxial cable to a δ-function at t_o has been investigated by Wiginton and Nahman[3] and is of the form

$$g(t,t_o) = \frac{1}{\sqrt{\pi}\ s} \left(\frac{s}{t-t_o}\right)^{3/2} e^{-s/t-t_o} \qquad t > t_o ,$$

$$= 0 \qquad t < t_o , \quad (11)$$

where

$$s(\text{nsec}) = \frac{10.12 \times 10^{-5}\ \xi^2\ L^2}{f(\text{MHz})} \quad .$$

ξ is the cable attenuation in dB per 100 ft measured at a frequency f, and L is the cable length in feet.

If the impulse is $S(t_o-\tau)$, then the output of the bridge to first order is

$$V_c(t) = \frac{V_o\ K}{4\ Z_o} \int_0^\infty S(t_o-\tau)\ g\ (t,t_o-\tau)\ d\ t_o \quad , \qquad (12)$$

where K is the conversion that relates the resistance change to the stress on the gauge.

Equation 12, in principle, relates an arbitrary stress to the signal from the bridge observed at a later time. While in principle Eq. (12) can be inverted to obtain S knowing V_c, it is not often done. Instead, it is more usual to use better cable, to use compensated cable, or to restrict the frequency range of interest to such values that $g\ (t,t_o-\tau)$ is practically a δ-function.

III. DESIGN

Figure 3 shows a simplified diagram of the bridge. The floating power supply charges the capacitor C to voltage V_o. When required, a trigger pulse T fires the SCR switches. A pulse of $V_o/2$ is applied to the PRE, represented by R, and the voltage developed across it is compared with that developed across the resistor Z_o. The difference in potential is measured at R_T and presented to the recording equipment.

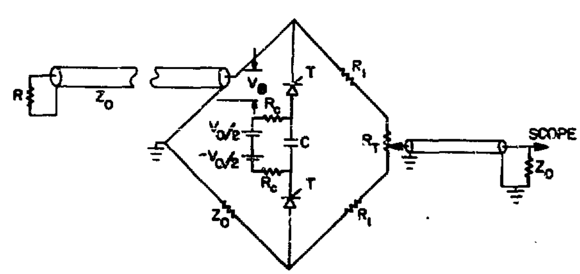

Fig. 3. Simplified bridge diagram.

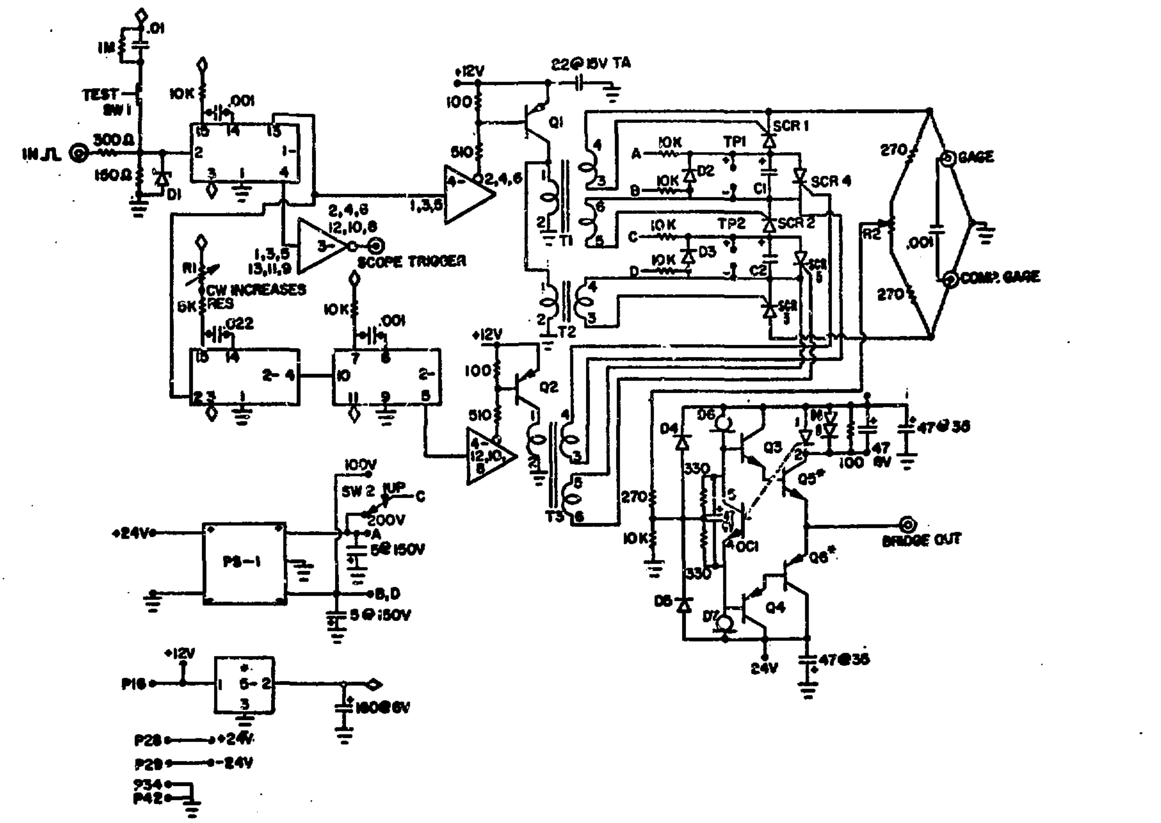

Fig. 4. Pulsed piezoresistive gauge bridge circuit. Components are: IC1,2: SN74123; IC3: MC7404; IC4: SN7406; IC5: LM309H; Q1,2,4: 2N3645; Q3: 2N3643; Q5: 2N3300; Q6: 2N3502; SCR1,...5: 2N4443; OC1: MCT2; PS-1: MIL PD16; R1: 100K Trimit; R2: 100Ω Trimit; C1,2: 70 mF @ 250V; D1: 1N4728A; D2,3,8,9: IN4005; D4,5: IN645; D6,7: IN5314; T1,2,3: Technitrol 11NGB.

The bridge itself has no characteristic impedance. Also, when the SCRs fire, the two halves of the bridge are electrically separated. Therefore, the resistors R_1 and R_T may be fairly large as long as the effects of stray capacity do not distort the signal output.

Referring to Fig. 4, an input pulse of +4 V, > 0.5 μsec, or pressing the "Test" pushbutton, triggers the monostable multivibrator IC1, whose time constant is set for 3 μsec output. This signal is coupled to IC4-1,3,5, an open collector inverter that drives Q1 to saturation, triggering SCR 1,2,3 and connecting the bridge to capacitors C1 and C2. When SW-2 is in the 200-V position, both capacitors are charged to 200 V through 10 kΩ resistors; when in the 100-V position only C1 is charged to 200 V. After the firing of the SCR, the bridge has a 400 or 200 V pulse across it with a decay constant of 3 msec. Since this is only a 3.2% droop in 100 μsec, it appears to be a flat pulse and, for most purposes, the droop needs no correction.

The negative output of IC1 is used by IC3 to provide a positive 3-V, 3-μsec pulse as a scope trigger while the positive output is used to trigger IC2-4, a monostable multivibrator whose time constant is externally adjustable from 45 to 650 μsec. The negative output of IC1 triggers IC2-5 when the pulse goes in a positive direction. This provides the necessary delay in the triggering of IC2-5 which produces a 3-μsec pulse that, after amplification, triggers SCR4 and 5, short circuiting capacitors C1,2 and terminating the pulse on the bridge.

The balance output of the bridge comes from R2 and goes to the bipolar output stage. Diodes D4, D5, and the 270-Ω resistor constitute limiters so that if the bridge is used improperly, or a gauge fails, the output stage will not be ruined. Transistor Q3 drives Q5 and Q4 drives Q6; however, this results in a voltage difference between the base of Q3 and Q4 of about 2.4 V if the transistors are to be conducting. (If they are not normally conducting, the driver is highly nonlinear for small signals.) The necessary offset voltage is provided by the constant current diodes D6 and D7 with the voltage developing across the series 330-Ω resistors. Ordinarily this would result in excessive current flow if the voltage were not regulated by the optically coupled pair OC1, the phototransistor of which shunts the two 330-Ω resistors, and the photodiode senses the current flowing in Q5 and Q6. The diodes D8 and D9 protect the photodiode from large currents and the 47-μf capacitors slow the reaction time constant to 31 msec. The 100-Ω resistor shunting the photodiode establishes the steady current in the driver.

This output circuit works very well, producing an output of ± 22 V on 50 Ω, using a supply voltage of only ± 24 V. Its risetime was measured as 5 nsec and the gain is 0.95; above ± 10 V the gain of the driver increases to 0.96. The output impedance is about 2 Ω.

This circuit is layed out on a printed-circuit board using ground-plane techniques and is installed in a single-width 8 3/4-in. NIM module (see Fig. 5). Table I summarizes the significant parameters.

Fig. 5. Pulsed piezoresistive gauge bridge.

IV. PERFORMANCE

Figure 6 shows the gauge output voltage when operating in the 200-V position; the comparison output looks the same except it is negative. Figure 7 shows the bridge balanced with 50 Ω precision film resistors on the bridge arms. In these tests, problems were encountered with sparking in the metal film resistors and with resistor heating. It seems that composition carbon resistors are free of both of these problems but the resistors must be selected for value if some precision is desired.

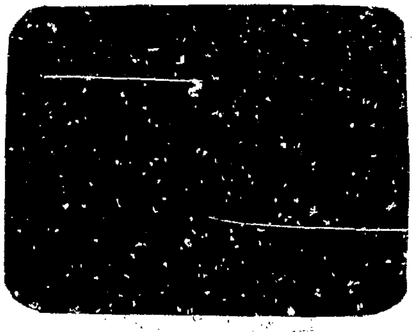

Fig. 6. Voltage pulse at the gauge connection. Scope settings: 50 V/cm, 20 μsec/cm.

TABLE I

PARAMETERS OF THE PULSED PIEZORESISTIVE GAUGE BRIDGE*

Pulsed voltage on piezoresistive element..	200 or 100 V switch selected
Power requirements....	+ 12V:137 mA; + 24V:98 mA; - 24V:29 mA
Triggering...........	External + 4 V, > 3 μsec pulse; manual
Scope trigger.........	+ 3 V, 3 μsec on 50 Ω
Bridge pulse	
Time duration.......	45-650 μsec front panel screwdriver adjustment
Rise time...........	200 nsec
Fall time...........	1 μsec
Delay time..........	400 nsec
Noise in output.......	± 2.5 mV
Balance adjustment range.................	± 10%
Test points..........	Monitor the voltage on each capacitor
Recharge time.........	6.4 sec to 99%

*input protected.

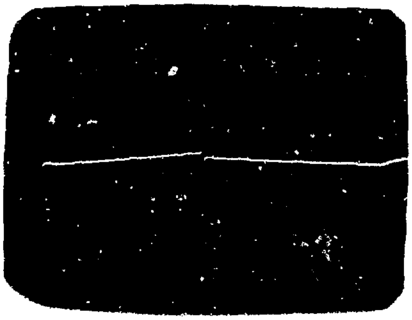

Fig. 7. Bridge output at balance. Scope settings: 0.5 V/cm, 20 μsec /cm.

Fig. 8. Bridge output with 50 and 56.2 Ω as the gauge and comparison gauge. Scope settings: 5 V/cm, 20 μsec/cm.

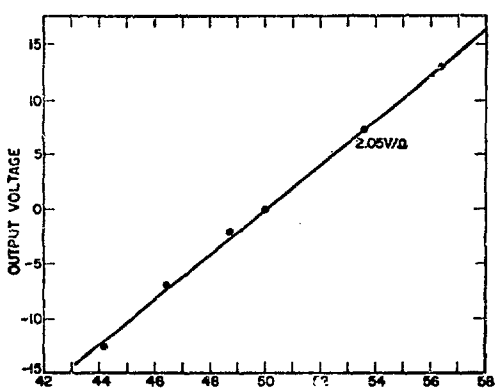

Fig. 9. Comparison of measured bridge output and calculated output.

In Figs. 7 through 16, the bridge output was terminated in 51 Ω at the oscilloscope.

Figure 7 shows the bridge output when 50 Ω resistors are connected as the gauge and comparison gauge and the bridge is adjusted for best balance. The shift corresponding to 1/8 Ω change in 100 μsec is probably due to unbalanced resistor heating. With this balance, but with resistors of 50 and 56.2 Ω respectively, the bridge output is shown in Fig. 8.

Using a succession of resistance values, a graph of output voltage (terminated in 50 Ω) vs resistance is obtained as shown in Fig. 9. Also plotted is a straight line of slope 2.05 V/Ω which is the sensitivity given by Eq. (10) using $Z_o = 50$ Ω and $V_o = 410$ V, the sum of voltages measured at the test points. Therefore it is apparent that this bridge does not need to be calibrated; its sensitivity may be calculated by knowing the charging voltage and the comparison resistance.

The foregoing statements are correct for the bridge alone, but when used asymmetrically, i.e. with a manganin gauge connected to the bridge by a long, lossy transmission line and the other side of the bridge resistively terminated, the output shows pronounced effects. Figure 10 shows the filling-time effect in 1000 ft of RG 214/U coaxial cable. The convex leading edge of the trace shows that the impedance of the cable increases as the wave travels. If the effect were this simple, it would just be a straight-line increase. However, as the impedance increases due to the resistance of the cable, it reflects back a fraction of the signal which rounds the ramp into the curve shown. When the wave arrives at the 50 Ω termination this effect no longer continues, but the high impedance is partly due to skin effect and must decay to the dc impedance. As the cable settles into a steady-state condition, the resistance observed at the bridge is the sum of the dc cable resistance and the termination, i.e. 3.26 + 50 Ω. Figure 10 indicates 3 Ω as the steady-state resistance. During the initial filling surge, the impedance rose to a peak of 5.5 + 50 Ω.

In practice, it is not desirable to measure the signal on a 5-V pedestal; instead, the bridge is rebalanced so that the steady-state voltage including the cable resistance is at the base line. Figure 11

Fig. 10. Effect of cable filling time. Scope settings: 5 V/cm, 20 μsec/cm.

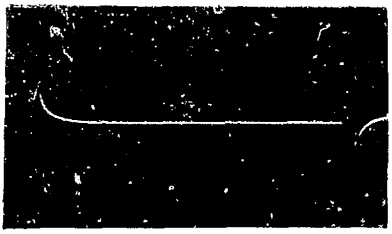

Fig. 11. Balanced bridge with 1000 ft of RG 214/U coaxial cable terminated in 50 Ω connected as the gauge. Scope settings: 5 V/cm, 10 μsec/cm.

Fig. 12. Balanced bridge with 1000 ft of RG 214/U coaxial cable terminated in 56.2 Ω connected as the gauge. Scope settings: 5 V/cm, 10 μsec/cm.

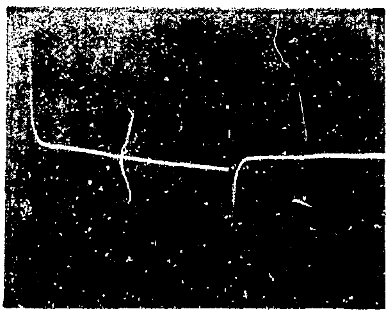

Fig. 13. Balanced bridge with 1000 ft of RG 214/U coaxial cable terminated in a 50-Ω manganin gauge. Scope settings: 5 V/cm, 10 μsec/cm.

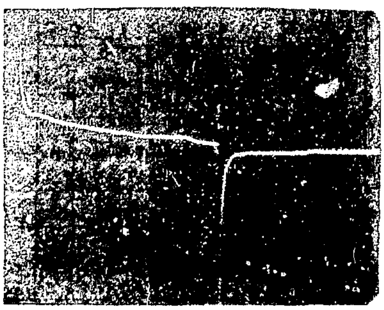

Fig. 14. Balanced bridge with 1000 ft of RG 214/U coaxial cable terminated in a 50-Ω manganin gauge impacted by a 4-lb hammer. Scope settings: 5 V/cm, 10 μsec/cm.

shows the output when the bridge is so adjusted. This is followed by connecting 56.2 Ω to the long transmission line as shown in Fig. 12.

Next a 50-Ω manganin gauge is connected to the long transmission line (see Fig. 13) and, when not stressed, shows an impedance of 50.2 Ω, dropping with time to 49.8 Ω. This slope is probably due to heating. Figure 14 shows the output when the gauge is struck with a 4-lb hammer. This signal is believed to be the dying tail of the impact but the gauge failed before the timing could be adjusted to catch the initial rise.

The way to avoid this filling-time transient is to use an equal line on the other side of the bridge and the effects will cancel. Figure 15 shows the signal at balance when 1000 ft of RG 214/U coaxial cable terminated in 50 Ω is connected to both sides of the bridge. Figure 16 shows the effect of terminating the comparison line in 56.2 Ω. Note that the use of two lines has cancelled out the filling transient, but there is the usual high-frequency degradation due to the long transmission line.

Fig. 15. Cable filling-time effect compensated by 1000-ft RG 214/U coaxial cables on both bridge arms and terminated in 50 Ω. Scope settings: 5 V/cm, 20 μsec/cm.

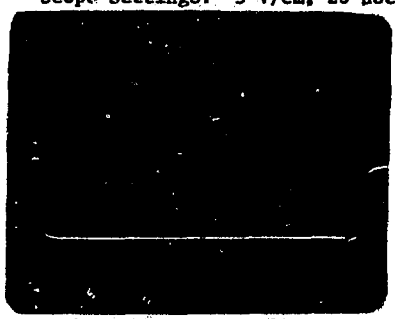

Fig. 16. Cable filling-time effect compensated by 1000 ft of RG 214/U coaxial cables on both bridge arms. Bridge cable is terminated in 50 Ω; compensation cable is terminated in 56.2 Ω. Scope settings: 5 V/cm, 10 μsec/cm.

V. CONCLUSIONS

The pulsed bridge described here is an improvement over those previously used. At present the 50 nsec risetime is satisfactory for the field measurements but future needs may require a coaxial-like layout of components, high-frequency compensation of the bridge output arm, and isolation of the capacity of the coupling transformers.

VI. BIBLIOGRAPHY

1. L. Costrell, "Standard Nuclear Instrument Modules", National Bureau of Standards report, TID-20893 (Rev.) (1966).

2. R. R. Fullwood, "AEC Standard Modules for Field Instrumentation", Los Alamos Scientific Laboratory report LA-4041 (1969).

3. R. L. Wiginton and N. S. Nahman, "Transient Analysis of Coaxial Cables Considering Skin Effect", Proc. I.R.E. 45, 166 (1957).

CM/ad:327 (50)